Journal of Solid State Chemistry **155,** 286–291 (2000)
doi:10.1006/jssc.2000.8886, available online at http://www.idealibrary.com on IDEAL®

Low-Temperature Phase Transition and Structural Relationships of $(CH_3NH_3)_3Bi_2Cl_9$

I. Belkyal,* R. Mokhlisse,† B. Tanouti,† K.-F. Hesse,‡ and W. Depmeier‡

*Faculté des Sciences et Techniques, Département Chimie, Univ. Cadi Ayyad, B.P. 618, Marrakech, Morocco; †Faculté des Sciences, Département Chimie, Univ. Cadi Ayyad, B.P. S15, Marrakech, Morocco; and ‡Institut für Geowissenschaften, Universität zu Kiel, Olshausenstr. 40. D-24098, Kiel, Germany

Received November 5, 1998; in revised form July 12, 2000; accepted July 27, 2000; published online November 29, 2000

$(CH_3NH_3)_3Bi_2Cl_9$ exhibits two phase transitions at $T_{c_1} = 349$ K and $T_{c_2} = 247$ K. The upper transition is probably isomorphous and reveals itself by the anomalous evolution of the lattice parameters. This behavior is explained to be due to increasing thermal motion of the methylammonium cations. The space group in both phases is *Pnma*. Single crystal X-ray work performed at 215 K indicates $P2_12_12_1$ as probable space group for the low-temperature phase with $a = 20.43(1)$, $b = 7.644(3)$, $c = 13.225(4)$ Å, and $Z = 4$. Symmetry analysis allows one to ascribe nearly tricritical character to the low-temperature phase transition. Structural relationships of $(CH_3NH_3)_3Bi_2Cl_9$ are displayed in the form of a group–subgroup diagram.

Key Words: **ferroelastoelectric character; tricritical character.**

INTRODUCTION

Tris(methylammonium)nonachlorodibismuthate (III), $(CH_3NH_3)_3Bi_2Cl_9$, is a representative of a family of layered compounds with the general formula $[NH_{4-n}(CH_3)_n]_3M_2X_9$, where M = Sb, Bi and X = Cl, Br, I. The systematic exchange of both organic and inorganic constituents within this family has yielded several compounds with interesting polar properties and numerous phase transitions (1, 2). The title compound (abbreviated MACB) crystallizes at room temperature in the orthorhombic space group *Pnma*, $Z = 4$ (3–6). The structure is formed by infinite $Bi_2Cl_9^{3-}$ polyanions which form zig-zag double-chains running along [010] (5, 6). The chains are connected by three crystallographically independent $CH_3NH_3^+$ cations. Alternatively, the structure can be regarded to consist of layers formed by $CH_3NH_3^+$ cations and Cl^- anions, the stacking direction being parallel to [100]. The Bi^{3+} ions occupy exclusively Cl^- coordinated octahedral voids in this packing.

The study of the phase transitions occurring in MACB, together with previously published data (3, 4), leads to a puzzling situation. Two phase transitions at $T_{c_1} = 349$ K and $T_{c_2} = 247$ K were detected by means of differential scanning calorimetry (DSC) measurements (3). The transition at T_{c_1} is accompanied by anomalies in the thermal evolution of lattice parameters and of the dielectric constant. The transition at T_{c_2} cannot be detected by either of these techniques, but was unambiguously disclosed by means of ^{209}Bi NQR (nuclear quadrupole resonance) experiments (7).

The aim of the present paper is to report the results of a structure examination of MACB at low temperature, to provide some facts about the character of the phase transition at T_{c_2}, and to propose phase relationships based on group–subgroup considerations.

EXPERIMENTAL

The crystal that was used earlier for the determination of the room temperature structure (6) was again used in this experiment. It measured $0.532 \times 0.076 \times 0.076$ mm^3, and data were collected on a Siemens AED2 four-circle diffractometer using graphite-monochromatized Mo$K\alpha$ radiation ($\lambda = 0{,}71069$ Å), in the θ–2θ scan technique. The range of 2θ was 1.5°–50°; the range of h, k, l was $-9/9$, $-15/15$, $-24/23$. The intensities of 3731 reflections were recorded; 2381 had $I > 3\sigma(I)$ and were used for the subsequent structure refinement. Crystal data are as follows: orthorhombic, space group $P2_12_12_1$, $a = 20.43(1)$, $b = 7.644(3)$, $c = 13.225(4)$ Å, $V = 2065(2)$ Å^3, $F(000) = 1432$, μ(Mo$K\alpha$) = 18.17 mm^{-1}, $T = 215$ K. The unit cell dimensions were refined using 20 reflections in the range $15° < 2\theta < 25°$. Lorentz, polarization, and absorption corrections were applied (Siemens software: REDU4, EMPIR). The positions of the nonhydrogen atoms were determined by direct methods (SHELXS-86 (8)). Anisotropic temperature parameters were used for Bi, Cl atoms; individual isotropic temperature parameters were applied to C, N atoms. The refinement was carried out by full-matrix least-squares methods using the program SHELXS-93 (9). The atomic scattering factor for neutral atoms Bi, Cl were taken from (10) and for C and N from (11). Refinement converged at $R_1 = 0.049$

0022-4596/00 $35.00

($R_1 = \sum||F_o| - |F_c||/\sum|F_o|$) for 2381 reflections with $I > 3\sigma(I)$, and 0.088 for all 3731 data. The latter value reflects the high number of weak reflections. $wR_2 = 0.146$ ($wR_2 = [\sum[W(F_o^2 - F_c^2)^2)/(n-p)]^{1/2}$, where n is the number of reflections and p is the total number of parameters refined). Weights were calculated according to $w = 1/\sigma^2(F_o^2)$. Maximum and minimum heights in the final difference Fourier map were 4.20 and -3.61 eÅ^{-3}, both close to the Bi atoms.

X ray powder diffraction measurements were performed on a Guinier HUBER G645 diffractometer, equipped with a closed-cycle He-cryo-refrigerator (CTI cryogenics). Cu$K\alpha_1$ radiation ($\lambda = 1.5406$ Å) from a doubly bent Johansson monochromator was used and detected by a scintillation counter. The sample was mounted vertically in the vacuum sample chamber and moved horizontally during the measurements in order to improve the counting statistics. The temperature stability was about 0.1 K. Silicon was used as internal standard. Data were collected in the step-scanning mode with a step width of 0.05° 2θ and a constant time of 60 s for each step. The 2θ range was 10°–60°. Lattice constants were refined by the least-squares method using the program Pulver (12).

The temperature dependence of the optical birefringence $\Gamma(T)$ was determined at 546.1 nm with an Ehringhaus compensator and a heating and cooling stage (THM 600 Linkam Sci. Instr. Ltd., Waterfield, UK), mounted on a Leitz polarizing microscope. To minimize the error of the measured values, ten readings of the optical path difference were performed. The uncertainly of the birefringence Δn was estimated to be three times that of the optical path difference, because of the error in the determination of the thickness of the sample.

RESULTS AND DISCUSSION

Symmetry Analysis of the Phase Transitions

The examination of a MACB single crystal made with a polarizing microscope along the three crystallographic directions did not reveal any change of the principal axes of the refractive indices through the two phase transitions, and no ferroelastic domains occurred. Furthermore, the intensity distribution of the X-ray diffraction pattern presented no fundamental change when examined at different temperatures employing an Imaging Plate system. Hence, it is concluded that the orthorhombic system is preserved throughout the sequence of phase transitions. The different phases are designated OHT (orthorhombic high temperature), ORT (orthorhombic room temperature), and OLT (orthorhombic low temperature).

The ORT → OLT phase transition has been detected by means of DSC measurements reported earlier (3) with a small sharp peak at T_{c_2} exhibiting features characteristic of a specific heat anomaly C_p. This transition was also

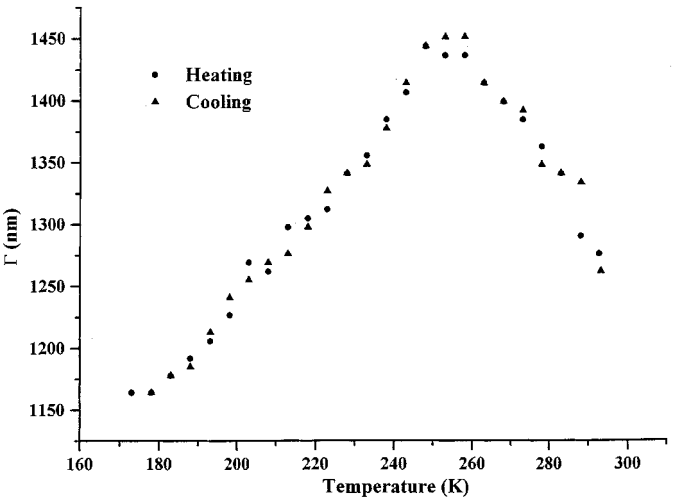

FIG. 1. Temperature dependence of the optical path difference in the $(CH_3NH_3)_3Bi_2Cl_9$ crystal.

unambiguously seen by means of measurements of the optical path differences $\Gamma(T)$ on a MACB crystal. The corresponding curve recorded on heating and cooling runs between 180 and 300 K is presented in Fig. 1. A distinct thermal anomaly which is perfectly reproducible and reversible appears around T_{c_2} with a small hysteresis. From the experimental evidence it can be concluded that this phase transition is second order or very nearly so. As mentioned above, the electric permittivity shows no anomaly at T_{c_2}. Together with the results of the optical examination, this allows one to conclude that this transition is neither ferroelastic nor ferroelectric.

From these characteristics and employing the tables of isotropy subgroups (13), $P2_12_12_1$ can be found as the possible space group for the OLT phase. The occurrence of several reflections with (0kl): $k + l \neq 2n$ and (hk0): $h \neq 2n$ in the data collected at 215 K is in full agreement with this assignment, as these reflections are systematically extinct in space group *Pnma* of ORT, but allowed in $P2_12_12_1$. The temperature dependence of the intensity of the (023), (032), and (520) reflections across T_{c_2} is shown in Fig. 2. The power law behavior of the intensities is obvious.

The noncentrosymmetric space group $P2_12_12_1$ is a maximal subgroup of *Pnma* of type translationengleich and index 2 ($t2$). The transition *Pnma* → $P2_12_12_1$ results in a secondary ferroic which is classed as "ferroelastoelectric." The two equivalent types of domains of the low-temperature phase could potentially be switched by simultaneous application of elastic stress and an electrical field. The phase transition is driven by the one-dimensional irreducible representation Γ_1^-/A_u of *Pnma* at the center of the Brillouin zone. The Landau condition is fulfilled and a second order character of the transition possible. This would agree with our DSC

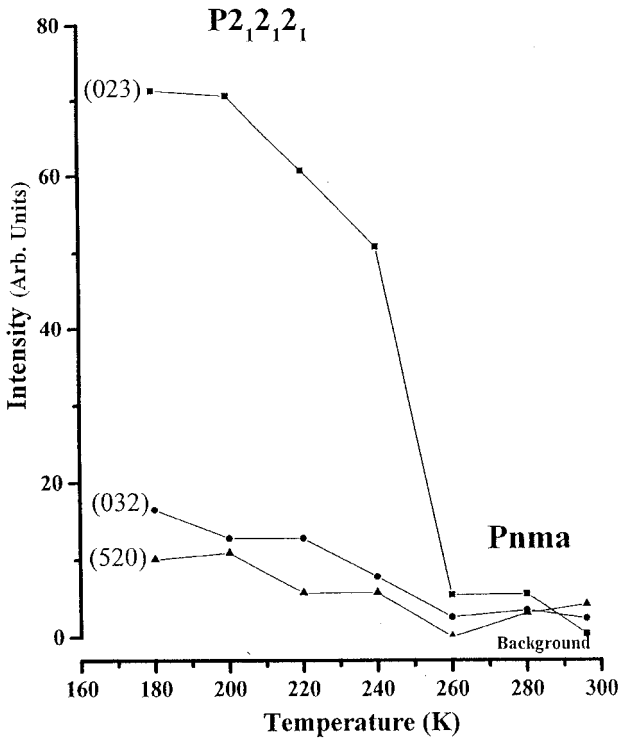

FIG. 2. Thermal evolution of the intensity of the (023), (032), and (520) reflections. The estimated uncertainly is 3% for all experimental points.

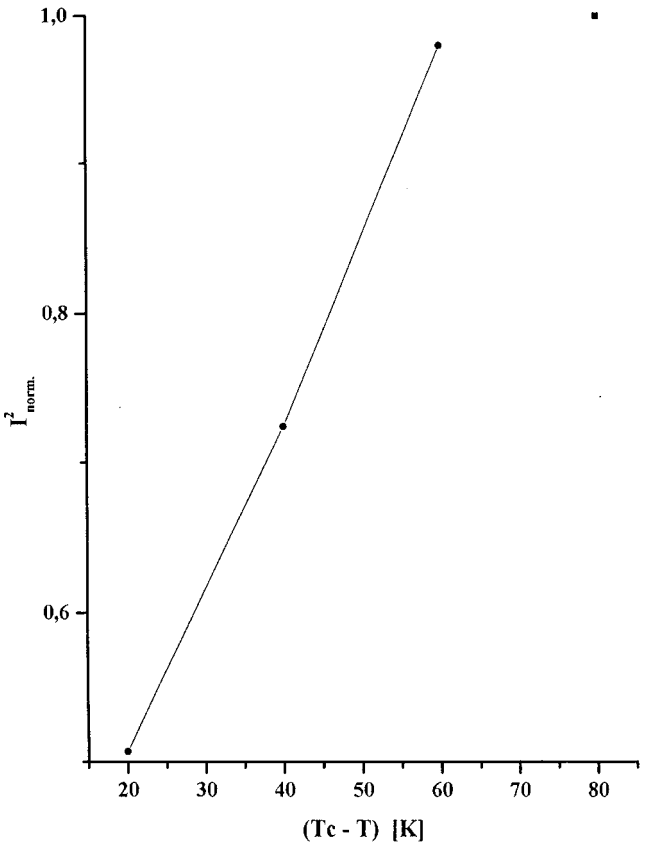

FIG. 3. Variation of the intensity squared of the (023) reflection versus $(T_c–T)$ in the OLT phase.

and optical measurements. However, the results of the NQR spectroscopic experiment (7) showed a discontinuity, indicative of a first order character of the transition. This apparent contradiction can be reconciled if a nearly tricritical character for the phase transition is assumed.

The Landau potential of a tricritical phase transition can be written,

$$\phi(\eta) = 1/2\, A_o(T - T_c)\eta^2 + 1/6\, D\eta^6 + \ldots,$$

where the coefficients A_o and D are > 0, and T_c is the transition temperature. The solution for this 2–6 potential yields $\eta = \pm [A_o/D(T_c - T)]^{1/4}$, for $T < T_c$.

The order parameter is thus proportional to $(T_c - T)^{1/4}$. This implies a linear variation of the reflection intensity squared versus $(T_c - T)$. Figure 3 demonstrates that this is, indeed, the case. The intensities were normalized with respect to the 167 K data. The deviation from linearity far away from the transition is assumed to be due to saturation of the order parameter.

The specific heat ΔC_p for a tricritical phase transition is proportional to $(T_c - T)^{\alpha}$, with $\alpha = 0.5$. By plotting $\log(\Delta C_p)$ versus $\log(T_c - T)$ measured in a former DSC experiment (3), we could demonstrate that this is fulfilled (see Fig. 4). Thus, the experimental data on MACB agree with the assumption of a tricritical character of the ORT → OLT phase transition. More precise measurements would probably reveal a weakly first-order character, as discussed by Hüller and Press (14). Such detailed investigations were beyond the scope of the present experiment.

The high-temperature ORT → OHT phase transition was disclosed by means of dielectric measurements (3). The DSC measurement was less clear as it yielded a complex-shaped signal (3). The transition becomes also noticeable by strong shifts of the positions of X-ray powder diffraction lines around T_{c_1}. Precession and Weissenberg photogrpahs of MACB single crystals confirm the variation of the lattice parameters above T_{c_1}. No change could be detected with respect to the systematic extinction rules. Both *Pnma* and $Pn2_1a$ obey the same reflection conditions. If the transition was assumed to involve a change $Pnma \rightarrow Pn2_1a$ with an ensuing appearance of an electrical polarization, the static electric permittivity could be supposed to follow a Curie–Weiss law on both sides of the transition temperature . In (3) it was shown that the experimental data do not agree with such an interpretation. Thus, on the basis of the presently available experimental results, one is led to the conclusion that the OHT and ORT phases belong both to the same space group, *Pnma* with $Z = 4$. The ORT → OHT phase transition is therefore regarded as isomorphic

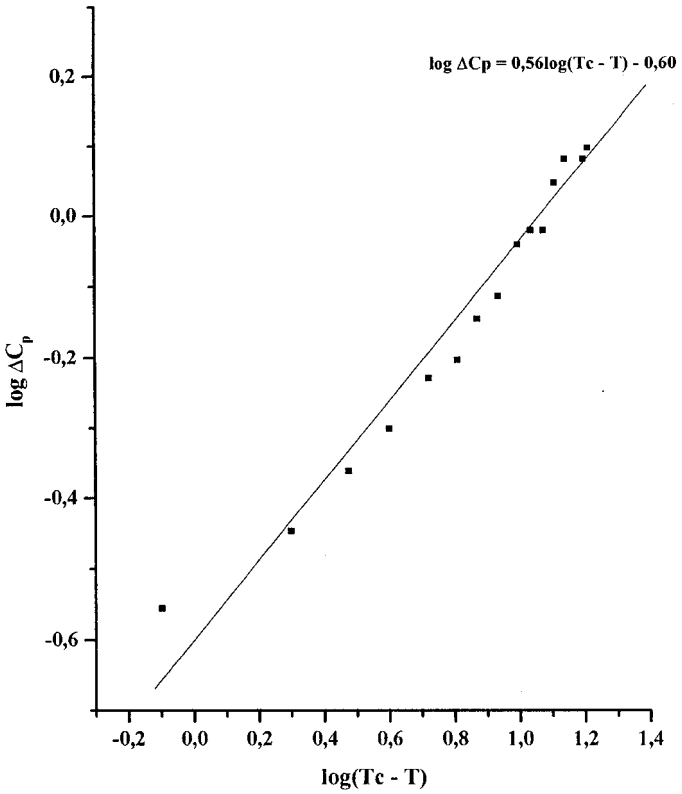

FIG. 4. Linear regression of log ΔC_p versus $\log(T_c - T)$ across the ORT → OLT phase transition.

(equisymmetric). Application of the Landau theory of phase transition (15) reveals that isomorphic transitions are necessarily of first order, because of the existence of cubic invariants in the Landau potential.

The Structure of the OLT Phase

The structure of the OLT phase is very similar to that of the ORT phase at room temperature (5, 6). Even by careful inspection no differences between the structures at 293 and 215 K could be detected that exceed the corresponding estimated standard deviations. Therefore, the atomic coordinates, anisotropic and isotropic thermal parameters of all atoms, interatomic distances, and angles are not given here, but have been deposited as supplementary material, as well as a figure showing the structure.

The isotropic atomic displacement parameters determined at 293 K (6) and 215 K allow one to calculate an average thermal amplitude of the atoms, viz. ≈ 0.26 Å and ≈ 0.23 Å at 293 and 215 K respectively. Obviously, the atomic static displacements resulting from the ORT → OLT phase transition are hidden by the dynamic effects and remain therefore undetectable within the precision of the present diffraction experiment. The phase change $Pnma \rightarrow P2_12_12_1$ corresponds to the loss of mirror planes in the OLT phase with an antisymmetric displacement of some mirror-related atoms. It is assumed that this is due to changes within the hydrogen bonding system. The atomic displacements induce the formation of ferroelastoelectric domains in the OLT phase. The existence of twin domains has been confirmed by the refined value (0.47) of the Flack parameter (16).

The Temperature Dependence of Lattice Parameters

The lattice parameters *a*, *b*, and *c* and the unit cell volume of MACB normalized to the values at 225 K are plotted versus temperature in Fig. 5. The temperature dependence of the lattice parameters around the ORT → OLT phase transition at 247 K is weak. However, a strong contraction of the *a* parameter and simultaneous expansion of the *b* and *c* parameters are clearly observed above the ORT → OHT transition temperature at 349 K. The unit cell volume is virtually unaffected by this phase transition.

From the crystal structure determination at room temperature it is known that the methylammonium cations point with their long axes almost along the *a* axis (5, 6). This results in an *a*-lattice parameter which is about 9.3% longer than the corresponding value of the isostructural $Cs_3Bi_2Cl_9$ (17), but practically unchanged *b* and *c* parameters. The observed thermal evolution of the lattice parameters above the ORT → OHT transition can consistently be explained by increasing inclination of the C–N vectors away from the *a* axis and toward the *b* and *c* axes due to increasing thermal motion.

Structural Relationships

The crystal structure of MACB can be schematized by … ABACBC … sequences of layers consisting of $CH_3NH_3^+$ cations and Cl atoms. The stacking direction is the [100] axis. The Bi atoms occupy those octahedral voids between these layers which are coordinated by Cl atoms only (5, 6). This arrangement would be ideally closed packed, if the $CH_3NH_3^+$ cations and the Cl atoms were assumed to be identical. The … ABACBC … sequence composed of identical spheres corresponds to the … hcc … Jagodzinski (18), or … + + + − − − … (or 33) Zhdanov (18) notation. The analysis of the latter symbol allows us to find $P6_3/mmc$ as the space group of the ideal structure (19).

For the ideal hexagonal closest packing (hcp), the a_{hcp} and c_{hcp} lattice parameters are related by $a_{hcp}/c_{hcp} = 1.633$. If all atoms were supposed to have the size of the Cl atoms, the lattice parameters can be estimated: $a_{hcp} = 2r_{Cl^-} \approx 3.6$ Å and $c_{hcp} \approx 5.9$ Å. For the ABACBC sequence, the c_{ABACBC} parameter along the stacking axis is three times that of the hcp, hence $c_{ABACBC} = 3c_{hcp} \approx 17.7$ Å. The a_{ABACBC} parameter is doubled with respect to hcp, if an

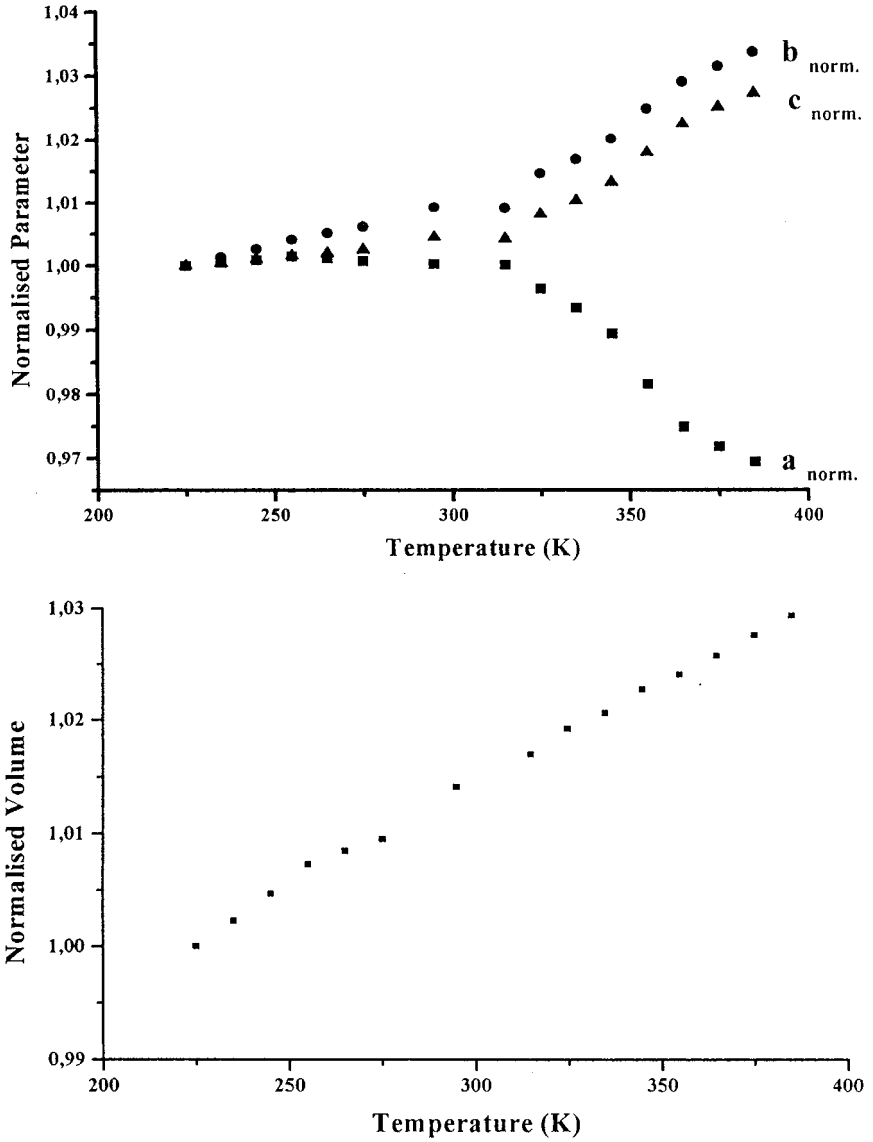

FIG. 5. Temperature dependence of the lattice parameters of $(CH_3NH_3)_3Bi_2Cl_9$.

ordering as observed in MACB of two types of equally sized atoms in the layers is considered: $a_{ABACBC} = 2a_{hcp} \approx 7.2$ Å. For the corresponding orthohexagonal/orthorhombic lattice (*Cmcm*), the b_{ABACBC} parameter calculates $b_{ABACBC} = \sqrt{3}a_{ABACBC} \approx 12.5$ Å. Hence, the ABACBC lattice parameters are in the *Cmcm* notation: $a \approx 7.2$, $b \approx 12.5$, and $c \approx 17.7$ Å. Transformed to *Amma* this becomes $a \approx 17.7$, $b \approx 7.2$, and $c \approx 12.5$ Å. These values are in good agreement with those found at room temperature for $Cs_3Bi_2Cl_9$ ($a = 18.684(4)$, $b = 7.644(3)$, and $c = 13.227(3)$ Å) (17) and MACB ($a = 20.426(2)$, $b = 7.700(1)$, and $c = 13.249(2)$ Å) (3, 4). The elongation of the a lattice parameters in MACB has been explained above.

Figure 6 illustrates the symmetry relations for MACB according to the Bärnighausen scheme (20), with the ideal hexagonal closest packing of spheres on top of the diagram, and the symmetry reduction broken down into smallest steps of group–maximal subgroup relations. For each such step, it is indicated whether the relation is of type "isomorphic" (i), "klassengleich" (k), or "translationengleich" (t), followed by the index of the corresponding group–subgroup relation. The number of possible domain orientations corresponds to the respective index. Transformations of the unit cell and origin shifts are also given, if appropriate. The temperature and character of the two phase transitions are also indicated in the diagram.

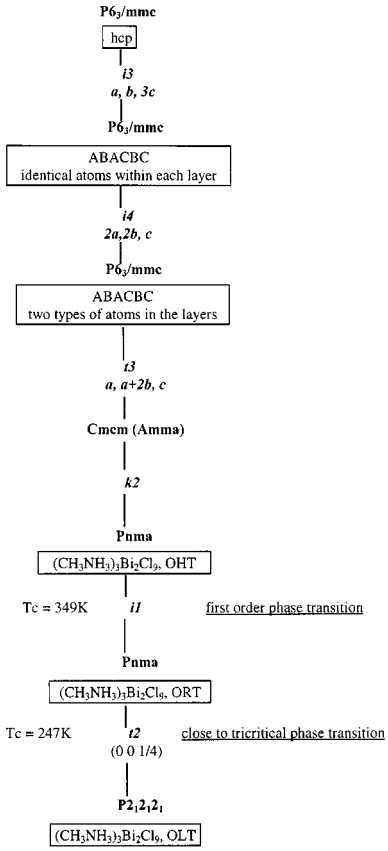

FIG. 6. Group–subgroup relations of the $(CH_3NH_3)_3Bi_2Cl_9$ phases, and the relationship with the hexagonal closest packing of identical spheres. The relationships are characterized by "i" or "t" or "k" and the corresponding index. "i" or "t" or "k" indicate whether the group–subgroup relationship is of type isomorphic, translationengleich, or klassengleich (21), respectively, while the index indicates the number of possible domain orientations.

CONCLUSION

The orthorhombic system is preserved throughout the two phase transitions of MACB: ORT → OHT at $T_{c_1} = 349$ K and ORT → OLT at $T_{c_2} = 247$ K. The ORT → OHT transition has been observed by DSC, dielectric, and X-ray powder diffraction measurements (3). The temperature dependence of the lattice parameters indicates an evolution around T_{c_1} explained by increasing inclination of the C–N bond of the $CH_3NH_3^+$ cations due to increasing thermal motion. The ORT → OLT transition has been disclosed by DSC measurements (3), NQR spectroscopy (7), and also by optical measurements reported here.

In agreement with the experimental results, the structural analysis performed at 215 K leads to $P2_12_12_1$ as the probable space group for the OLT phase. It follows that the ORT → OLT transition is potentially of ferroelastoelectric character. Since the room temperature space group is conserved in the OHT phase, the ORT → OHT transition is of isomorphic type. The experiments suggests a nearly tricritical character for the low-temperature transition and first order for the high temperature transition.

An ideal hexagonal structure is found when the $CH_3NH_3^+$ cations are supposed to be identical with the chlorine atoms.

SUPPORTING INFORMATION AVAILABLE

Tables of crystallographic details, fractional atomic coordinates, anisotropic and isotropic thermal parameters of all atoms, interatomic distances, and angles for $(CH_3NH_3)_3Bi_2Cl_9$ at 215 K are available from the authors.

ACKNOWLEDGMENTS

We thank Mrs. P. Herms for the optical measurements and the Deutsche Forschungsgemeinschaft for a grant which made the stay of one of us (I. Belkyal) in Kiel possible.

REFERENCES

1. R. Jakubas, J. Zaleski, and L. Sobczyk, *Ferroelectrics* **108,** 109 (1990).
2. P. E. Tomaszewski, *Phys. Stat. Sol.* (*b*) **181,** 15 (1994).
3. I. Belkyal, R. Mokhlisse, B. Tanouti, N. B. Chanh, and M. Couzi, *J. Alloys Compounds* **188,** 186 (1992).
4. I. Belkyal, R. Mokhlisse, B. Tanouti, N. B. Chanh, and M. Couzi, *Phys. Stat. Solid.* (*a*) **136,** 45 (1993).
5. I. Belkyal, R. Mokhlisse, B. Tanouti, K.-F. Hesse, and W. Depmeier, *Zeit. Kristallogr.* **212,** 139 (1997).
6. I. Belkyal, R. Mokhlisse, B. Tanouti, K.-F. Hesse, and W. Depmeier, *Ann. Chim. Sci. Matér.* **23** (1–2), 203 (1998).
7. H. Ishihara, K. Watanabe, A. Iwata, K. Yamada, Y. Kinoshita, T. Okudo, V. G. Krishnan, Shi-Qi Dou, and A. Weiss, *Z. Naturforsch. A* **47,** 65 (1992).
8. G. M. Sheldrick, "SHELXS-86, Program for Crystal Structure Determination," Univ. of Göttingen, Germany, 1986.
9. G. M. Sheldrick, "SHELXL-93, Program for Crystal Structure Determination," Univ. of Göttingen, Germany, 1993.
10. "International Tables for X-Ray Crystallography," Vol. IV. Kynoch Press, Birmingham, 1974.
11. D. T. Cromer and J. B. Mann, *Acta Crystallogr. A* **24,** 321 (1968).
12. K. Weber, Auswertung von Pulverdiagrammen PC-VERS, 1991.
13. H. T. Stokes and D. M. Hatch, "Isotropy Subgroups of the 230 Crystallographic Space Groups," World Scientific, Singapore, 1988.
14. A. Hüller and W. Press, *in* "The Plastically Crystalline State-Orientationally-Disorderedcystals," (J. N. Sherwood, Ed.), Wiley, New York, 1979.
15. J. C. Toledano and P. Toledano, "The Landau Theory of Phase Transitions," p. 172–176, World Scientific, Singapore, 1987.
16. H. D. Flack, *Acta Crystallogr. A* **39,** 876 (1983).
17. K. Kihara and T. Sudo, *Acta Crystallogr. B* **30,** 1088 (1974).
18. M. O. Keeffe and B. G. Hyde, "Crystal Structures I. Patterns and Symmetry," Mineralogical Society of America, 1996.
19. Th. Hahn, "International Tables for Crystallography, Vol. A. Space Group Symmetry," 2nd revised ed., Reidel, Dordrecht, 1987.
20. H. Bärnighausen, *Acta Crystallogr. A* **31,** S3 (1975).
21. H. Wondratschek, *in* "International Tables for Crystallography, Vol. A. Space Group Symmetry," (Th. Hahn, Ed.), 2nd revised ed., pp. 709–734. Reidel, Dordrecht, 1987.